III International Conference on Particle-based Methods – Fundamentals and Applications
PARTICLES 2013
M. Bischoff, E. Oñate, D.R.J. Owen, E. Ramm & P. Wriggers (Eds)

NUMERICAL INVESTIGATION ON UNSTEADY VORTICAL FLOWS WITH A GRID-FREE VORTEX METHOD

KOTA FUKUDA[1]

[1] School of Engineering
Department of Aeronautics and Astronautics
Tokai University
4-1-1 Kitakaname, Hiratsuka-city, Kanagawa, 259-1292, JAPAN
e-mail: fukuda@tokai-u.jp, web page: http://www.ea.u-tokai.ac.jp/fukud

Key words: Vortical flow, Turbulent flow, Vortex method, Grid-free Simulation.

Abstract. In this study, a grid-free vortex method was developed and applied to turbulent flows in order to validate the scheme. In order to satisfy the boundary condition for internal flow calculation, the direct boundary element method (BEM) was employed. The grid-free redistribution model proposed by Fukuda and Kamemoto [3] and vortex reconnection model was also introduced and the spatial resolution was improved for high strain regions. From the results, it was confirmed that the unsteady feature of the turbulent boundary layer in the turbulent internal flow and its development were successfully captured. Furthermore, comparisons of the calculated mean velocity and the calculated rms value of the axial velocity fluctuation in the turbulent internal flow with experimental data showed that the method provided an accurate velocity profile and axial velocity fluctuation in turbulent boundary layers. In the vortex rings interaction calculation, reconnection process was reasonably simulated and the spatial resolution was improved even in the high strain regions using the redistribution model and the reconnection model. The analysed energy spectra were in close agreement with the existing DNS and experimental data up to high wave number regions.

1 INTRODUCTION

One of the crucial problems for turbulent flow analyses via computational fluid dynamics (CFD) is how to analyze the unsteady motion and deformation of vortical structures. The Navier-Stokes flow solvers with the finite element method (FEM), the finite difference method (FDM), or the finite volume method (FVM) can capture the vortical structures explicitly, but when the computational grid is not sufficiently small, the vortices are diffused due to the numerical diffusion.

In the vortex methods, vorticity distributions in the flow fields are represented by using discrete vortex elements and the motion and evolution of vorticity of each element are calculated at each time step. When compared to other computational schemes, vortex methods have the advantage that the nonlinear distortion of vortical structures is directly calculated without the numerical diffusion.

The vortex methods are divided into two types of methods by the scheme of calculation of the velocity field. The first one is vortex-in-cell (VIC) method. The stream function is calculated on the fixed grid, and the velocity is computed by finite differences on the grid.

Another is the vortex method based on the Biot-Savart law, in which the velocity field is calculated by the Biot-Savart law, without using the computational grid.

In the vortex methods, numerical resolution is dependent on the scale of the discrete vortex elements. When the size of the elements approaches the Kolmogorov dissipation scale, the calculation becomes Direct Numerical Simulation (DNS) of turbulence. The scale range between the largest and smallest scale of vortical structure is locally different especially in turbulence. Therefore, the local redistribution scheme is necessary for high strain regions. Cottet et al. [1] calculated two fundamental turbulent flows by the VIC method, which incorporated a grid-base redistribution model. The results indicated that the energy spectra by the vortex method were close to those by DNS. On a grid-free redistribution model for vortex method based on the Biot-Savart law, Nakanishi and Kamemoto [2] proposed the 3-D core spreading method, in which each vortex element is replaced into a vortex blob element at each time step. In high strain regions, however, the spatial resolution becomes worse because the distance of each element becomes larger than its core radius of the element. Fukuda and Kamemoto [3] proposed a different type of grid-free redistribution model, in which each vortex element is split into some elements according to the stretching rate of each element. The redistribution model was applied to the simulation of the collision of two vortex rings. The results showed that the analyzed energy spectra were in good agreement with existing DNS data and results of experiments and the energy cascade mechanism was reasonably simulated. The great advantage of the vortex method incorporating with the grid-free redistribution model is that it can be easily applied to the flows with complex geometry because of its grid-free characteristic. The scheme has been applied into the various engineering problems (see, for example, [4-6]). However, there are few studies on the validation as DNS or large eddy simulation (LES) scheme.

In this study, the grid-free vortex methods including the grid-free redistribution model and vortex reconnection model was applied a turbulent flows in order to validate the scheme for numerical simulation of turbulent flows.

2 NUMERICAL METHOD

2.1 VORTEX METHOD

In the vortex methods, vorticity distributions in the flow field are represented by using discrete vortex elements. The governing equation is the vorticity transport equation and the pressure poisson equation, which is can be derived by taking rotation and divergence of the Navier-Stokes equations, respectively.

$$\frac{\partial \boldsymbol{\omega}}{\partial t} + (\mathbf{u} \cdot grad)\boldsymbol{\omega} = (\boldsymbol{\omega} \cdot grad)\mathbf{u} + \upsilon \nabla^2 \boldsymbol{\omega} \tag{1}$$

$$\nabla^2 P = -\rho div(\mathbf{u} \cdot grad \mathbf{u}) \tag{2}$$

where $\boldsymbol{u}$ is a velocity vector and the vorticity $\boldsymbol{\omega}$ is defined as $\boldsymbol{\omega} = \mathrm{rot}\ \boldsymbol{u}$. In the vortex methods, the time evolution of the flow is represented by the motion and evolution of vorticity strength of each element.

In this study, the stretch term and diffusion term in the equation (1) were separately considered and the viscous term was expressed by the core spreading method proposed by

Leonard [7]. The velocity filed was determined by the Biot-Savart law as explained by Wu and Thompson [8].

$$\mathbf{u} = \int_V \boldsymbol{\omega}_i \times \nabla_i G dV + \int_S \left[\left(\mathbf{n}_j \cdot \mathbf{u}_j \right) \cdot \nabla_j G - \left(\mathbf{n}_j \times \mathbf{n}_j \right) \times \nabla_j G \right] dS \tag{3}$$

Here, subscription *i* indicates variable or differentiation at the flow field and subscription *j* denotes the ones at the boundary surface. $\boldsymbol{n}$ is the normal unit vector and ∇ is the gradient operator. *G* is the fundamental solution of the scalar laplace equation. In the three dimensional flows, *G* is written as

$$G = \frac{1}{4\pi \left| r - r_i \right|} \quad or \quad G = \frac{1}{4\pi \left| r - r_j \right|} \tag{4}$$

In this study, the vortex tube model was employed as discrete vortex element. The trajectories of the discrete elements over each time step was computed by using the third order Adams-Bashforth method.

In order to obtain boundary variables for turbulent internal flow calculation, which satisfy the boundary condition, the direct BEM was employed. The inlet and outlet boundary conditions were imposed by the inlet and outlet velocity profile. On the boundary condition for the wall surface, the wall normal velocities were set as zero by the BEM and the non-slip condition on the wall surface was satisfied by using linear vortex panels based on the method proposed by Ojima and Kamemoto [9]. The vorticity field near the wall surface can be represented by the proper distributions of the vortex panels and vortex elements introduced into the flow field. The discrete vortex elements were introduced into the flow field from the surface vortex panels at each time step by considering their convective and diffusion velocities based on the method proposed by Ojima and Kamemoto [9].

2.2 GRID-FREE REDISTRIBUTION METHOD

In this study, the grid-free redistribution method [3] for vortex elements was employed and the spatial resolution was improved for high strain regions. When the stretch term in the equation (1) is larger than the viscous term, the ratio of the length to the core radius of each vortex element becomes large. In the redistribution model, each discrete element is replaced by some elements according to its deformed length and radius and therefore the spatial resolution is improved in high strain regions. In this study, an element was divided into two elements when the ratio of the length to the diameter became more than two. The detail of the grid-free redistribution method is can be found in Fukuda and Kamemoto [3]. Furthermore, in this study, vortex reconnection model was introduced and the numerical simulation was accelerated using the GPUs.

3 CALCULATION CONDITIONS

In this study, turbulent internal flow calculation and simulation of two vortex rings interaction were carried out. For the turbulent internal flow calculation, experimental results by Durst et al. [10] and Toondera et al. [11] were used to compare the present numerical results. The computational parameters were set based on the experimental condition: The Reynolds number based on the bulk velocity U_b and the pipe diameter *D* were set to be

$\mathrm{Re}=U_b D/\nu=10{,}000$, which corresponded to $\mathrm{Re}_\tau=U_\tau D/\nu=620$. The length L of the pipe was taken $L=20D$. The tube was represented by 1,600 surface triangle panels as shown in Figure 1. The time step sizes was set to be $\Delta t = 0.01D/U_b$. The vorticity layer thickness on the wall boundary was set as $h/D=0.001$. In this study, inlet and outlet boundary conditions were set, instead of periodic boundary condition in order to simulate time evolution of the boundary layer from the initial state.

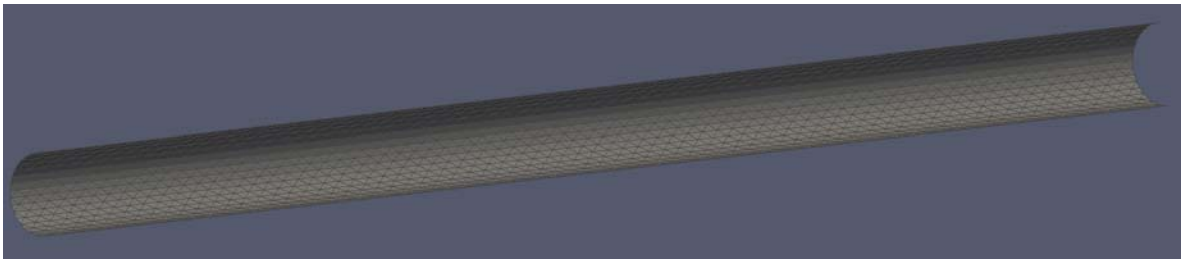

Figure 1: Surface triangles for turbulent internal flow calculation.

For vortex rings interaction, the vortex ring parameter and initial setup of the vortex rings are consistent with one of the study by Knio & Ghoniem [12]. The vortex ring parameter and initial setup of the vortex rings are as Table 1. Here, r is the position on the cross section. Γ_0 and R_0 are the circulation on the cross section and the core radius of the vortex ring at the initial state respectively. The time step was chosen as $\Delta t=0.02R_0^2/\Gamma_0$.

Table 1: Vortex rings parameter at the initial state

Ring circulation Γ_0	2.0
Core radius of vortex ring δ_0/R_0	0.275
Reynolds number $Re_\Gamma 0=\Gamma 0/\upsilon$	2200
Inclined angle θ	30°
Distance of two rings D	$3.0R_0$

4 RESULTS AND DISCUSSIONS

4.1 TURBULENT INTERNAL FLOW

4.1.1 TRANSITIONING BOUNDARY LAYER

In the present calculation, unsteady evolution of the vertical structure in the pipe was directly simulated from the initial state. Figure 2 shows the instantaneous distribution of the discrete vortex elements at the half length of the pipe. The flow direction is from left to right. From the result, it was confirmed that the flow state was initially laminar and the unsteady feature of the turbulent boundary layer and its development were successfully captured. Furthermore, comparison between the results with and without the grid-free redistribution model showed that the fine eddy structures generated from the larger scale structures in high strain regions were reasonably captured using the redistribution model.

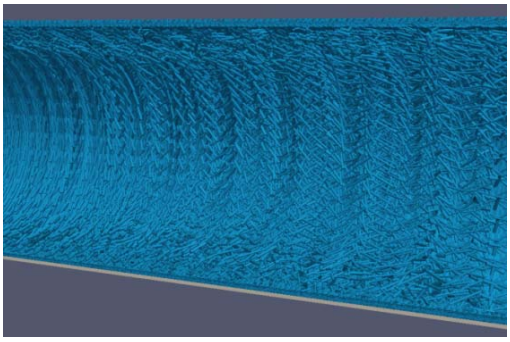

Figure 2: Vortex element distribution at the half length of the pipe.

4.1.2 MEAN VELOCITY PROFILE

Figure 3 shows the mean velocity profile normalized by the wall shear stress velocity as a function of the distance to the wall in wall units y^+. The experimental data taken by Durst et al. [10] at Re=U_bD/ν=10,000 and taken by Toondera et al. [11] at Re=U_bD/ν=24,580 are plotted in the figure. The law-of-the wall, $u^+ = y^+$, and the logarithmic law, $u^+ = 2.5\ln(y^+) + 5.5$, are also included in the figure. The result showed the current result was in good agreement with the experimental data taken by Durst et al. [10] and Toondera et al. [11]. It can be confirmed from the result that the present method provided an accurate velocity profile in the turbulent boundary layers.

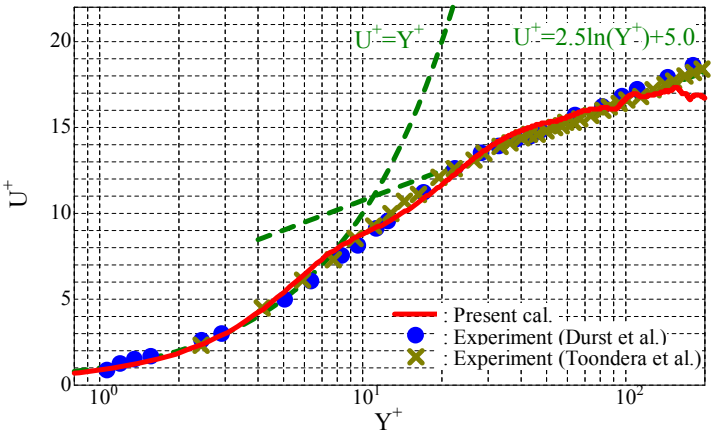

Figure 3: Mean velocity profile
(Dashed lines are linear and log law profile.)

4.1.3 RMS STATICS

The rms value of the axial velocity fluctuation is depicted in Figure 4. The experimental data taken by Toondera et al. [11] at Re=U_bD/ν=24,580 are plotted in the figure. From the experiments [11], it was confirmed that the axial rms profile does not show Reynolds number

effect up to y^+=30. The present results showed that the overall profile of the calculated rms value and the amplitude were close to the experimental data, even though the peak location of the calculated rms value slightly shifted to higher y^+ region.

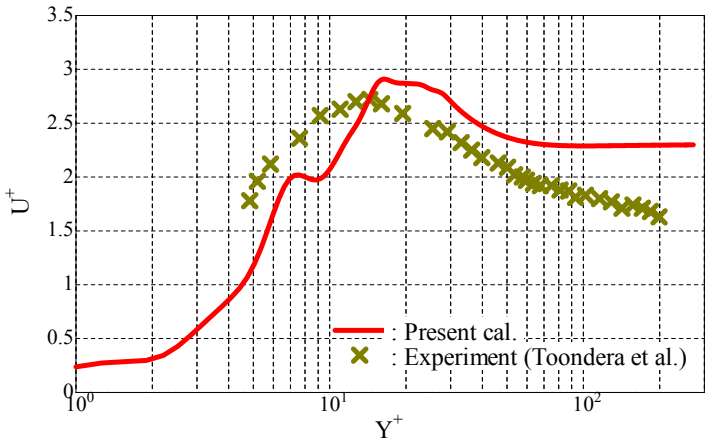

Figure 4: RMS value of axial velocity fluctuation

4.2 VORTEX RINGS INTERACTION

Figure 5 shows the instantaneous flow patterns calculated by the redistribution model and the vortex reconnection model. Each vortex ring approached by a self-induced velocity from the initial state and collided with each other. The result showed that the reconnection process was reasonably simulated and the spatial resolution was improved even in the high strain regions using the redistribution model and the reconnection model. Figure 6 shows the one-dimensional longitudinal power energy spectra based on the Kolmogorov universal scale calculated using the redistribution model and both the redistribution model and the vortex reconnection model, respectively. The analyzed energy spectra were in close agreement with the existing DNS and experimental data up to high wave number regions. Especially with both the redistribution model and the vortex reconnection model, the calculation provided more accurate energy spectra.

Figure 5: Instantaneous flow patterns

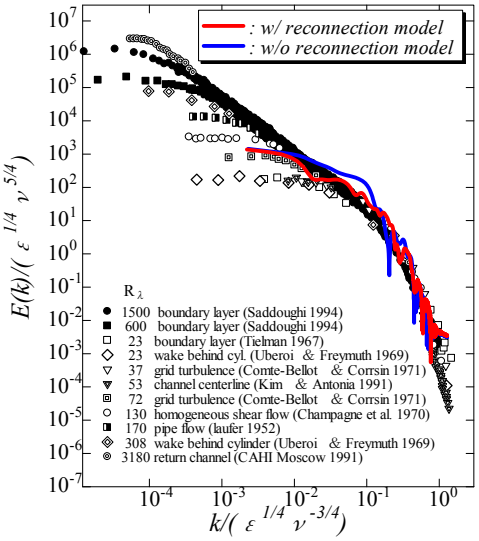

Figure 6: Analyzed energy spectra

5 CONCLUSIONS

In this paper, a grid-free vortex method combined with the direct BEM method and the grid-free redistribution model [3] was applied to the simulation of a turbulent pipe flow in order to examine the applicability of the scheme for turbulent internal flows and validate the scheme. Furthermore, vortex rings interaction was calculated with the grid-free redistribution model and the vortex reconnection model in order to validate the scheme.

In the turbulent internal flow calculation, comparisons of the calculated mean velocity and experimental data taken by Durst et al. [10] and Toondera et al. [11] showed that the method provided an accurate velocity profile in turbulent boundary layers and a clear view of the transition and unsteady characteristics of turbulent boundary layer. It was also confirmed that the redistribution model was effective to represent the deformation and evolution of vortical structures in high strain regions. Furthermore, comparison of the calculated rms value of the axial velocity fluctuation with experimental data taken by Toondera et al. [11] showed that the overall profile of the calculated rms value and the amplitude were close to the experimental data, even though the peak location of the calculated rms value slightly shifted to higher y+ region.

In the vortex rings interaction calculation, reconnection process was reasonably simulated and the spatial resolution was improved even in the high strain regions using the redistribution model and the reconnection model. Furthermore, the analysed energy spectra were in close agreement with the existing DNS and experimental data up to high wave number regions, especially with both the redistribution model and the vortex reconnection model.

From these results, it was confirmed that the vortex method incorporating with the grid-free redistribution model and vortex reconnection model is effective for the calculation of turbulent flows and unsteady evolution of turbulent vortical structure.

REFERENCES

[1] G. H. Cottet, B. Michaux, S. Ossia, and G. VanderLinden, *A Comparison of Spetral and Vortex Methods in Three-Dimensional Incompressible Flows*, Journal of Computational Physics, 175, 2002.

[2] Y. Nakanishi and K. Kamemoto, *Numerical Simulation of Flow around a Sphere with Vortex Blobs*, Journal of Wind Engineering and Industrial Aerodynamics, Vol. 46&47, pp.363- 369, 1992. K.

[3] Fukuda and K. Kamemoto, *Application of a Redistribution Model Incorporated in a Vortex Method toTurbulent Flow Analysis*, Proceedings of ICVFM2005, 2005.

[4] K. Kamemoto and A. Ojima, *A virtual wind tunnel for numerical simulation of flow-induced vibrations*, Proceedings of the 9th International Conference on Flow-Induced Vibrations, 2008.

[5] K. Kamemoto and A. Ojima, *Vortex method for the analysis of complex unsteady and vortical flows around a swimming fish*, Proceedings of the 3rd Int. Conf. Smart Materials, Structures and Systems, 2008.

[6] Y. Iso and K. Kamemoto, *A Grid-Free Lagrangian Approach of Vortex Method and Particle Trajectory Tracking Method Applied to Internal Fluid-Solid Two-Phase Flows*, Journal of Fluids Engineering, 130, 1, 2008.

[7] A. Leonard, *Vortex Methods for Flow Simulation*, Journal of Computational Physics, 37, 289, 1980.

[8] Wu, J. C., and Thompson, J. F., *Numerical Solutions of Time-Dependent Incompressible Navier-Storkes Equations Using an Integro-Differential Formulation*, Computers and Fluids, Vol.**1**, pp. 197–215, 1973.

[9] A. Ojima and K. Kamemoto, *Numerical Simulation of Unsteady Flows around Three-Dimensional Bluff Bodies by an Advanced Vortex Method*, JSME international Journal, 43-2, B, pp.127-135, 2000.

[10] F. Durst, J. Jovanovi´c, J. Sender, *LDA Measurements in the Near-Wall Region of a Turbulent Pipe Flow*, Journal of Fluid Mechanics, 295, pp. 305-335, 1995.

[11] J. M. J. den Toondera and F. T. M. Nieuwstadt, *Reynolds number effects in a turbulent pipe flow for low to moderate Re*, Phys. Fluids **9** (11), pp.3398-3407, 1997.

[12] Knio, O. M. and Ghoniem, A. F., *Numerical study of a three dimensional vortex method*, Journal of Computational Physics, Vol.86, pp.75-106, 1990.